The Circular Wire-Patch Resonator—Theory, Numerical Analysis, and Filter Design Application

Massimiliano Simeoni, *Member, IEEE*, Roberto Sorrentino, *Fellow, IEEE*, and Serge Verdeyme, *Member, IEEE*

***Abstract*—In this paper, a new type of microstrip resonator is presented, i.e., the circular wire-patch resonator. This component exhibits interesting electrical performances, including very compact dimensions and the possibility of high integration in multilayer low-temperature co-fired ceramic modules. For this new resonator, a transmission-line model, a finite-element-method analysis, and an application in filter design and some measurements are presented. Experimental results are discussed and compared with the theoretical and numerical ones showing a good agreement.**

***Index Terms*—Finite-element method (FEM), passive filters, patch resonator, Q factor, transmission-line theory.**

I. Introduction

COMPATIBILITY between planar circuits and monolithic microwave integrated circuits (MMICs) is a reason why it is very interesting to develop more compact and better performing passive microstrip components.

A very compact planar resonator useful to build low-temperature co-fired ceramics (LTCC) technology compatible low-loss microwave filters is presented in this paper.

Recently, Simeoni *et al.* [1], [2] presented a similar resonator (the rectangular wire patch) obtained by introducing a metallic post (via-hole) establishing an electrical connection between a microstrip patch and its ground plane. The insertion of the via-hole introduces a low-frequency resonance (compared to the fundamental resonance of the unperturbed patch), referred to here as "parallel resonance," a term already used in the antenna domain [3].

The present structure, the circular wire-patch resonator, is derived from the modification of the rectangular one. The new structure presents the advantage of a circular symmetry that enables the development of a theoretical model; the structure is shown in Fig. 1. The benefit of size reduction, observed for the squared resonator, is still present in the circular one.

Manuscript received June 3, 2002; revised September 3, 2002.

M. Simeoni was with the Institute of Research on Optical and Microwave Communications, University of Limoges, 87060 Limoges, France. He is now with the European Space Research and Technology Center, European Space Agency, 2200 AG Noordwijk, The Netherlands (e-mail: msimeoni@ieee.org).

R. Sorrentino is with the Department of Electronic and Information Engineering, University of Perugia, 06100 Perugia, Italy (e-mail: r.sorrentino@ieee.org).

S. Verdeyme is with the Institute of Research on Optical and Microwave Communications, University of Limoges, 87060 Limoges, France (e-mail: verdeyme@ircom.unilim.fr).

Digital Object Identifier 10.1109/TMTT.2003.809625

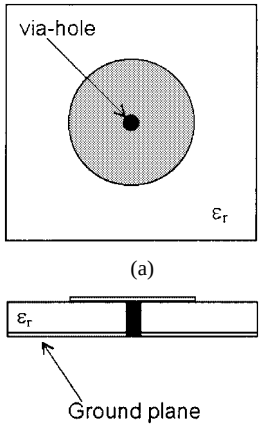

Fig. 1. Circular wire-patch resonator: physical structure. (a) Top view. (b) Side view.

The model, presented in Section II, is based on the theory of radial transmission lines and, via the solution of an eigenvalue equation, enables the analysis and synthesis of the resonator. End effects are taken into account. A theoretical estimation of the unloaded quality Q factor is obtained via the calculation of the electromagnetic (EM) energy stored inside the resonator and the average loss power (perturbation method). The theoretical results are presented, with the numerical and experimental ones, in Section IV. By performing a full-wave finite-element method (FEM) analysis of the embedded resonator (Section III), the distribution of the electric and magnetic fields inside the structure can be visualized and both the free and forced oscillation frequencies can be obtained. In Section IV, some experimental results are presented, showing the correct functioning of the resonator. Finally, in Section V, an example of bandpass filter design is presented. A filter for the Personal Handyphone System (PHS), a Japanese standard for personal mobile communications, has been synthesized. The design procedure results in a very compact structure: a two-pole filter having a central frequency of 1906 MHz is easily realized in a low-permittivity dielectric substrate $(\varepsilon_r = 2.32)$, having a surface of 7 cm $\times$ 4 cm.

II. Theory

A. Eigenvalue Equation

Let us consider a guiding structure composed by two conducting circular and parallel planes separated by a dielectric

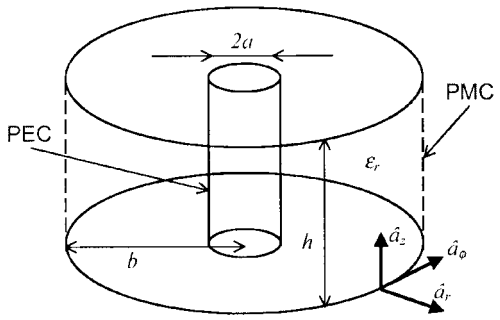

Fig. 2. Radial line model of the circular wire-patch resonator.

medium, this structure is known as a radial transmission line. The simplest propagating wave of this structure is a TEM wave propagating in the radial direction; the electric field is polarized in the axial direction and the magnetic field is purely circumferential. In the following discussion, a time factor $e^{j\omega t}$ will be assumed. Obviously there is not any radial component of the fields, the analytical expression of the $\overline{E}$ and $\overline{H}$ vectors in cylindrical coordinates is given by [4]

$$\overline{E} = E_z \hat{a}_z \tag{1}$$

$$\overline{H} = H_\phi \hat{a}_\phi \tag{2}$$

where

$$\begin{cases} E_z = AH_0^{(1)}(kr) + BH_0^{(2)}(kr) \\ H_\phi = \dfrac{j}{\eta}\left[AH_1^{(1)}(kr) + BH_1^{(2)}(kr)\right]. \end{cases} \tag{3}$$

$H_i^{(\nu)}(x)$ is the Hankel's function of the νth type $(\nu = 1,2)$ and ith order $(i = 0,1)$, k is the wavenumber. A and B are amplitude factors, $\eta = \sqrt{\mu/\varepsilon}$ is the wave impedance, and j is the imaginary unit.

The Hankel's functions are linear combinations of first- and second-kind Bessel's functions [$H_\nu^{(1)}(x) = J_\nu(x) + jN_\nu(x)$, $H_\nu^{(2)}(x) = J_\nu(x) - jN_\nu(x)$] [5]. Along the radial direction, the $H_n^{(1)}(kr)$ terms are identified as the negatively traveling wave, while the $H_n^{(2)}(kr)$ terms are identified as the positively traveling wave.

The circular wire-patch resonator can be seen as a radial transmission-line short circuited at $r = a$ [perfect electric conductor (PEC)] and opened at $r = b$ [perfect magnetic conductor (PMC)]; a and b are the radius of the via-hole and the patch, respectively (Fig. 2).

By applying the boundary conditions at $r = a$ and $r = b$ (the tangential component of the electric and magnetic fields are, respectively, equal to zero)

$$\begin{cases} E_z(kr)|_{r=a} = 0 \\ H_\phi(kr)|_{r=b} = 0 \end{cases} \tag{4}$$

we obtain

$$\begin{cases} AH_0^{(1)}(ka) + BH_0^{(2)}(ka) = 0 \\ AH_1^{(1)}(kb) + BH_1^{(2)}(kb) = 0. \end{cases} \tag{5}$$

We can write the system (5) in the form of a matrix equation

$$\begin{bmatrix} H_0^{(1)}(ka) & H_0^{(2)}(ka) \\ H_1^{(1)}(kb) & H_1^{(2)}(kb) \end{bmatrix} \cdot \begin{bmatrix} A \\ B \end{bmatrix} = \begin{bmatrix} 0 \\ 0 \end{bmatrix}. \tag{6}$$

The nonzero solutions are the roots of the following equation, i.e., the eigenvalue equation, obtained equalling to zero the determinant of the 2×2 matrix in (6):

$$H_0^{(1)}(ka)H_1^{(2)}(kb) - H_1^{(1)}(kb)H_0^{(2)}(ka) = 0. \tag{7}$$

The first value k_0 of k that satisfies the eigenvalue equation corresponds to the fundamental resonating mode of the structure.

The resonance frequency is calculated by

$$f_0 = \frac{k_0}{2\pi\sqrt{\varepsilon_r \varepsilon_0 \mu}}. \tag{8}$$

A simple program finding the roots of the eigenvalue (7) easily calculates the eigenvalue k_0.

B. End Effects

Equation (7) is based on the assumption that the electric field is purely vertical at the patch edges (electrical open-circuit assumption). A more accurate model must take into account the end effects generated by the abrupt termination of the guiding structure. The end effects are modeled by introducing an equivalent relative dielectric constant of the medium filling the space between the two conducting planes and an effective radius of the microstrip patch.

In the radial-line model, the electric field at the patch edges is assumed to be polarized in the z-direction and having no variations along the circumference of the patch, exactly the same peripheral distribution of the $\overline{E}$ vector at the edges of a circular microstrip disk capacitor. The equivalent relative permittivity of the dielectric medium and the effective radius of the patch can be calculated using the same equations used by Wolff and Knoppik [6] to characterize the effect of the fringing fields in the microstrip capacitors.

The equivalent relative dielectric constant $(\varepsilon_{\rm eq})$ is a function of the patch dimensions, substrate thickness (h), and relative dielectric constant of the substrate ε_r; the following expression can be used [6]:

$$\varepsilon_{\rm eq} = \frac{\dfrac{\varepsilon_0 \varepsilon_r \pi b^2}{h} + \left[\dfrac{1}{v_{ph}} Z(2b,h,t,\varepsilon_r) - \dfrac{2\varepsilon_0 \varepsilon_r b}{h}\right]\pi b}{\dfrac{\varepsilon_0 \pi b^2}{h} + \left[\dfrac{1}{c_0} Z(2b,h,t,\varepsilon_r = 1) - \dfrac{2\varepsilon_0 b}{h}\right]\pi b} \tag{9}$$

where v_{ph} is the phase velocity of a quasi-TEM wave on a microstrip line of width $2b$ and thickness t, on a dielectric substrate (ε_r) of thickness h.

v_{ph} is given by

$$v_{ph} = \frac{c_0 Z(2b,h,t,\varepsilon_r)}{Z(2b,h,t,\varepsilon_r = 1)} \tag{10}$$

where $c_0 = 3 \times 10^8$ m/s is the phase velocity of light in vacuum and $Z(2b,h,t,\varepsilon_r)$ is the characteristic impedance of a microstrip line of width $2b$ on a substrate (ε_r) of height h and metallization thickness t [7].

The effective radius of the patch [6] can be calculated by

$$b_{\rm eff} = b\sqrt{1 + \frac{2h}{\pi b}\left[\ln\left(\frac{\pi b}{2h}\right) + 1.7726\right]}. \tag{11}$$

It takes into account the electric and magnetic stray field of a resonator filled with a homogeneous medium $(\varepsilon_r = 1)$. Re-

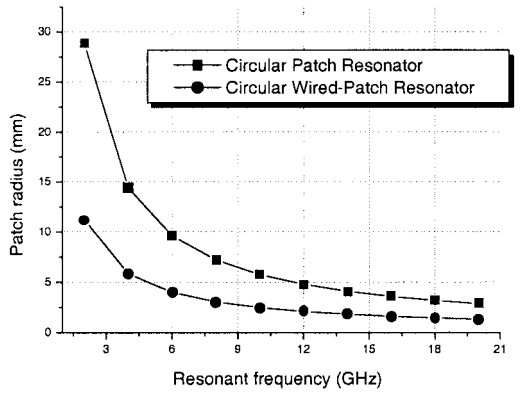

Fig. 3. Comparison between the patch radius of a standard circular patch resonator and the circular wire patch. The two resonators are printed on the same dielectric substrate (Duroid RT5870).

placing b with b_{eff} in (7), we are able to calculate k_0; using ε_{eq} at the place of ε_r, we can finally calculate the resonant frequency by (8).

The model can be inverted and used to synthesize a circular wire-patch resonator to produce a resonance at a given frequency. Fixing the characteristics of the substrate, the section of the via-hole and the value of the resonant frequency, we can automatically calculate the radius of the patch. Fig. 3 shows a comparison between the radius of a standard circular patch resonator and the radius of the circular wire patch; as a function of the resonant frequency. The curve relative to the standard circular patch has been drawn according to the analytical expression of the resonant frequency of its fundamental mode (TM_{110}) as given by Watkins [8]. The curve relative to the wire-patch is derived from the proposed model. The two resonators are printed on the same dielectric substrate (Duroid RT5870) having a relative dielectric constant of 2.32 and a thickness equal to 790 μm. The radius of the via-hole for the wire patch is 250 μm.

Using the circular wire-patch, an evident reduction of the patch radius can be achieved, particularly for relatively low resonant frequencies.

C. Loss Estimation

The loss estimation is based on the evaluation of the EM energy stored inside the resonator and the average power dissipation. The following definition of the Q factor is employed ([9, p. 314]):

$$Q = \frac{\omega(\text{ time–average energy stored in the system})}{\text{energy loss per second}}. \quad (12)$$

A first Q factor associated with the metallic losses and a second one associated with the dielectric losses are evaluated. The overall unloaded Q factor of the resonator is then deduced. The average energy W stored in the resonator is

$$W = W_{\text{electric}}|_{\max} = \frac{\varepsilon_0\varepsilon_{\text{eq}}}{2}\int_{\text{Volume}} |\overline{E}|^2 dV$$
$$= \frac{\varepsilon_0\varepsilon_{\text{eq}}}{2}\int_0^{2\pi}\int_0^{h}\int_a^{b_{\text{eff}}} |E_z|^2 r\,dr\,dz\,d\theta. \quad (13)$$

Since the expression of the electric field in known in an analytical form (3), the last integral can be easily evaluated.

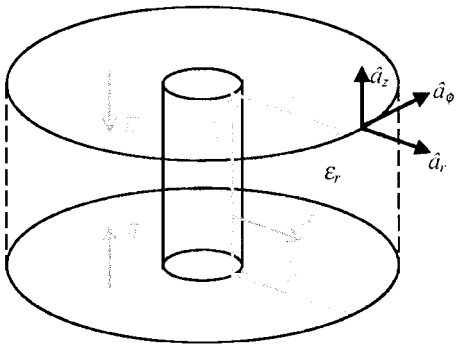

Fig. 4. Surface current distribution at the resonant frequency.

To evaluate the losses caused by the finite conductivity of the metallic walls, the surface currents $\overline{J_s}$ are first calculated. Knowing the tangential magnetic field at each metallic surface, $\overline{J_s}$ can be expressed as follows (for the lower plane, upper plane, and via-hole, respectively):

$$\overline{J_s} = -H_\phi \hat{a}_r \quad \overline{J_s} = H_\phi \hat{a}_r \quad \overline{J_s} = H_\phi|_{r=a}\hat{a}_z \quad (14)$$

where $\hat{a}_r$ and $\hat{a}_z$ are the unit vectors of the r- and z-axis. Fig. 4 shows the surface currents distribution.

The power loss in the metallic walls in given by

$$P_l = \frac{R_s}{2}\int_{\text{Metallic surfaces}} |\overline{J_s}|^2 dS$$
$$= \frac{R_s}{2}\left(\underbrace{2\int_0^{2\pi}\int_a^{b_{\text{eff}}} |H_\phi|^2 r\,dr\,d\theta}_{\mathbf{A}} + \underbrace{2\pi h a |H_\phi(r=a)|^2}_{\mathbf{B}}\right) \quad (15)$$

where $R_s = 1/\sigma\delta$ is the real part of the surface impedance of the metallic walls having σ conductivity and skin depth $\delta = (2/\omega\mu\sigma)^{1/2}$. $\mathbf{A}$ is the contribution to the losses associated with the patch and to the ground plane and $\mathbf{B}$ is the contribution to the losses associated with the via-hole.

The Q factors associated with the ohmic and dielectric losses are $Q_{\text{met}} = \omega W/P_l$ and $Q_{\text{diel}} = \varepsilon'/\varepsilon''$; where ε' and ε'' are, respectively, the real and imaginary parts of the permittivity of the dielectric medium filling the resonator.

The overall unloaded Q factor is

$$Q_0 = \left((Q_{\text{met}})^{-1} + (Q_{\text{diel}})^{-1}\right)^{-1}. \quad (16)$$

III. Numerical Analysis

A full-wave three-dimensional (3-D) EM analysis of the resonator has been performed using EMXD, an FEM software ([10, pp. 53–78]) developed at the Institute of Research for Optical and Microwave Communications (IRCOM), University of Limoges, Limoges, France. Both free oscillation and a forced oscillation (coupling the resonator to two microstrip lines) analysis have been performed by limiting the computational domain to within a metallic box.

Four different resonators have been dimensioned using our model to resonate at the frequency of f_0. The physical dimensions are summarized in Table I.

TABLE I
PHYSICAL DIMENSIONS OF THE PROTOTYPES

Res. n.	f_0 (GHz)	b (mm)	a (mm)	h (mm)	ε_r
1	2.40	9.46	0.250	0.790	2.32
2	5.80	4.14	0.250	0.790	2.32
3	2.40	8.90	0.400	0.780	3.20
4	0.68	27.89	0.400	0.780	3.20

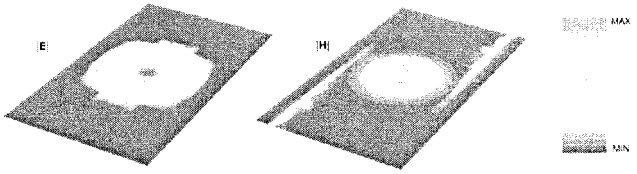

Fig. 5. Fields distribution at the resonant frequency (in a horizontal plane section at mid-height of the dielectric substrate).

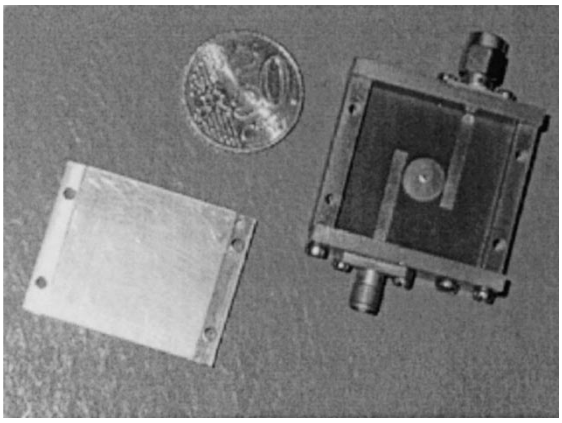

Fig. 6. One of the fabricated prototypes inside its shielding box (cover removed).

The actual sizes must be compared to the dimensions of the conventional circular-patch resonators resonating at the same frequencies [8]. The patch surface area is reduced approximately 6–7 times, with the presence of the via-hole, depending on the resonant frequency (see, for example, Fig. 3).

In the finite-element meshing, the circular patches have been approximated by polygons having 12 sides and perimeter length equal to the circumference of the patches. This approximation can lead to some differences between the numerical results and theoretical ones. A conductivity of 5.7×10^7 S/m is assumed for the patch and via-hole, an infinite conductivity is assumed for the shielding box. Dielectric losses are taken into account by means of the *tangent loss* of the medium.

The resonant frequencies and Q factors obtained by the FEM (free oscillations) analysis of the prototypes are only 1%–2% removed from the theoretical values. These results are presented, together with experimental measurements, in the Section IV. In order to compare the numerical results to some experimental data, we have analyzed the resonators by weakly coupling the single patch to a couple of microstrip lines and looking for a transmission peak associated with the resonance (forced-oscillation analysis). Two 50-Ω lines are coupled to the resonator simply by their proximity; the amplitude of the gap between the patch and lines changes the amount of these couplings. A gap of 300 μm is used for all the cases considered.

Fig. 5 shows the magnitude of the electric and magnetic field at the resonant frequency in a horizontal section of the structure.

According to the model, the magnitude of the electric field is mainly concentrated at the patch edges, where the magnitude of the magnetic field has a minimum. The maximum of the magnetic field around the via-hole is associated with the displacement current flowing through the metallic post. The electric current flowing in the microstrip lines is highlighted by the magnetic-field concentration below the conducting strips. The electric-field distribution suggests the possibility of coupling by proximity two or more resonators between them and to microstrip lines, enabling the synthesis of very compact planar filters.

Another interesting feature of the circular wire-patch resonator is the good frequency isolation of the "parallel resonance." The first higher order mode appears far enough from the fundamental resonance (at approximately $2f_0$) to permit the use of the resonator to synthesize wide-band spurious-free microwave filters.

IV. EXPERIMENTAL RESULTS

The prototypes presented in Table I have been realized and their performances measured on an HP8510 network analyzer. Fig. 6 displays one of the prototypes inside its shielding box.

The experimental estimation of both the resonant frequency and Q factor has been realized using a transmission-type technique [11]. The transmission coefficient ($|S_{21}|$) between the input and output ports is measured. The appearance of a transmission peak outlines the resonance of the component. By measuring the central frequency of that peak and its width, the resonant frequency and loaded Q factor associated with the resonance can be estimated. If the transmission lines are weakly coupled to the resonator, the value of the loaded Q factor is quite close to the value of the unloaded one, and the former value can then be used as a rough estimation of the latter. By measuring the level of insertion loss at the top of the peak ($|S_{21}(f_0)|$), one can calculate the coupling between the resonator and external circuit and, hence, derive the value of the unloaded Q factor. The weakness of the coupling between the resonator and microstrip lines increases the accuracy of the Q-factor estimation [12].

The theoretical, numerical, and measured values of both the resonant frequency and Q factor are summarized in Table II.

For the resonant frequency, we must compare the FEM free-oscillation (Fr.O.) values to the theoretical ones and the FEM forced oscillations (Fo.O.) to the measured ones. For the Q factor, we must compare the numerical results (Fr.O.) to the theoretical and measured values. Resonators 3 and 4 have been measured without any shielding box. They are then supposed to radiate a nonnegligible amount of power in the free space, in reason of the relatively large thickness and low permittivity of their substrates. Resonators 1 and 2 have been measured inside their shielding brass boxes. It should be noticed that the numerical analysis for each resonator has been conducted including the effect of the shielding cover.

For the resonant frequency, a very good agreement between theoretical, numerical, and experimental values can be noticed.

TABLE II
THEORETICAL, NUMERICAL, AND EXPERIMENTAL RESULTS

Res. n.	f_0 (GHz)				Q_0		
	Th.	FEM		Mea.	Th.	FEM	Mea.
		Fr.O.	Fo.O.			Fr.O.	
1	2.40	2.416	2.432	2.392	244	307	195
2	5.80	5.803	5.730	5.656	196	244	120
3	2.40	2.410	2.461	2.482	173	226	116
4	.680	0.698	0.686	0.675	129	204	84

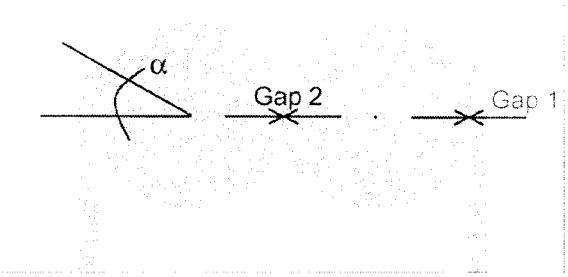

Fig. 7. Two-pole PHS filter layout.

The deviation between the theoretical and experimental values of the resonant frequency is the order of approximately 1% (consider, for instance, resonator 1). For the Q factor, the theoretical computations provide a rough estimation of the actual values. A bigger error is experienced for the unshielded resonators (resonators 3 and 4) since the radiation losses are nonnegligible in these cases.

V. FILTER DESIGN EXAMPLE

To demonstrate the possibility of integrating the circular wire-patch resonator in the passive microwave filter design, we focus on a specific application. The application considered is the PHS, a Japanese standard for personal mobile communications.

The PHS uses a filter with the following characteristics.

- Center frequency $=$ 1906 MHz.
- 3-dB bandwidth $=$ 27 MHz.
- In-band ripple $<$ 0.8 dB.
- In-band insertion loss $<$ 3 dB.

First, the dielectric substrate on which to print the circuit is selected. The RT/Duroid RT5870 (relative dielectric constant of 2.32 and thickness of 0.790 mm) has been chosen for reasons of price, availability, and mechanical properties.

The topology of the filter is very simple and consists of two identical circular wire-patch resonators, resonating on their parallel mode at the center frequency of the filter (1906 MHz). The resonators are mutually coupled by proximity and coupled, in the same manner, to two microstrip transmission lines. The in/out lines partially surround (for an angle α) the resonators in order to increase the amount of in/out coupling. Fig. 7 displays the filter layout (top view).

The first step is to empirically fix the coupling angle. Once fixed, the coupling angle α (30°), the width of the gap between the lines and the resonators (Gap 1) sets the proper value of the input coupling. The inter-resonators coupling is tuned by changing the width of the gap separating the two patches (Gap 2).

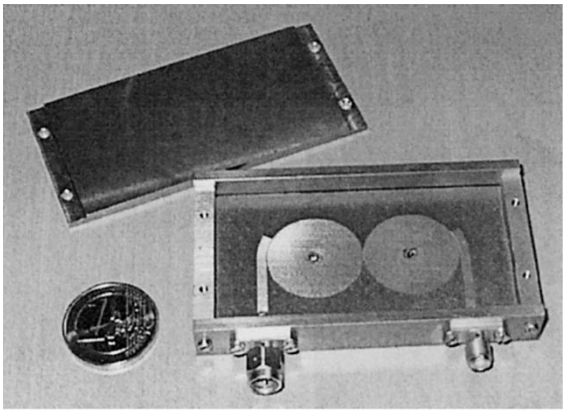

Fig. 8. PHS two-pole filter inside its shielding box (cover removed).

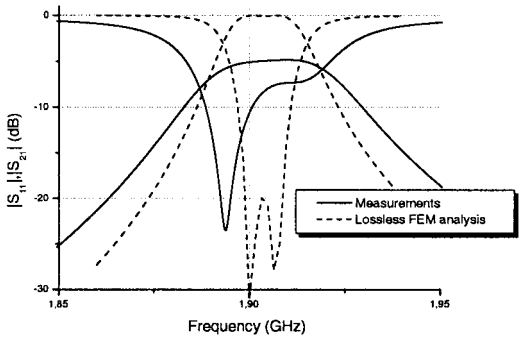

Fig. 9. Experimental (top cover on) and theoretical (lossless FEM) filter response.

The resonators are analytically dimensioned using the model presented in Section II. After a quick tuning, performed via a full-wave EM analysis (FEM), the design specifications are matched with a structure having the following dimensions.

- Patch radius (identical for both resonators) $=$ 11.80 mm.
- Via-hole radius (identical for both resonators) $=$ 250 μm.
- Gap-1 width $=$ 120 μm.
- Gap-2 width $=$ 60 μm.
- $\alpha = 30°$.

To stress that the optimization process has not affected the starting dimension of the patch radius, it results in a very quick design.

A prototype of the filter has been realized and measured inside its shielding brass box (included in the full-wave EM simulations).

Fig. 8 shows a photograph of the fabricated two-pole PHS filter.

Figs. 9 and 10 show the experimental results, in narrow-band and broad-band, respectively. An increase in the bandwidth (35 MHz instead of 27 MHz) and a consequential increase of the in-band reflection can be noticed. The insertion-loss level at the central frequency is approximately -3.8 dB. The central frequency is at 1907 MHz, which is only 1 MHz from the desired value.

The wide-band transmission confirms an excellent stopband rejection; a direct consequence of the very good frequency isola-

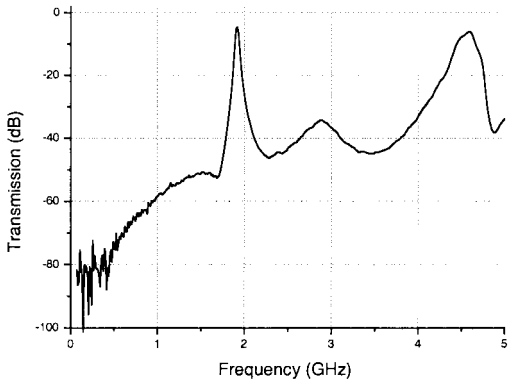

Fig. 10. Experimental broad-band filter response.

tion of the parallel resonant mode. The first higher transmission peak appears at approximately 4.5 GHz and is associated with the higher order resonance of the patches.

The excess in-bandpass and in-band insertion loss can be explained by the fact that the prototype has been realized with nonoptimum manufactory facilities. Uncertainty in the manufacturing tolerance of the gaps is the main problem that affects the realization. The imperfect connection between the silver-plated ground wire and the copper patch probably causes the excessive insertion loss. A continuous metallization for the patch and via-hole could probably reduce the ohmic losses, increase the unloaded Q factor of the resonator, and then reduce the filter insertion loss.

VI. Conclusion

A novel microwave resonator, the circular wire-patch resonator, has been introduced in this paper. The insertion of a metallic post establishing an electrical connection between a microstrip circular patch and its ground plane introduces a new low-frequency resonance. Just as in the case of the rectangular wire-patch resonator, presented in a previous paper, the resulting structure shows very compact dimensions associated with good electrical performances. The values of the unloaded Q factor for this new component are analogous at the case of classic microstrip patch resonators.

A radial transmission-line model enables the analytical (hence, virtually instantaneous) analysis and synthesis of the component. The realization of various prototypes has fully confirmed our model. The experimental results, especially for the resonance frequency, are in excellent agreement with the theoretical ones. The predicted value of the resonator's unloaded Q factor (obtained by a classical perturbation method) leads to a rough loss estimation. A numerical analysis (FEM) completes the investigation of the component.

A simple two-pole filter design has been presented in order to show the possible integration of this component in the passive filter design. The PHS (center frequency of 1906 MHz and bandpass of 27 MHz) has been selected as a potential application. Both narrow-band and broad-band measurements have been presented, confirming the potentialities of the resonator and displaying the very good stopband rejection of the filter. A better realization of the prototypes could surely lead to a finer agreement between the predicted and experimental behavior of the filter.

Acknowledgment

The authors wish to thank Dr. M. Dionigi, University of Perugia, Perugia, Italy, for his help in the realization and measurement of some of the prototypes.

References

[1] M. Simeoni, S. Verdeyme, D. Baillargeat, and P. Guillon, "Résonateur planaire compact pour des applications au filtreage microondes," in *Proc. Journées Nat. Microondes Conf.*, Poitiers, France, May 2001.

[2] M. Simeoni, S. Verdeyme, and P. Guillon, "Bandpass filter design using a novel compact planar resonator," in *Proc. 32nd Eur. Microwave Conf.*, Milan, Italy, Sept. 2002, pp. 733–735.

[3] C. Delaveaud, P. Léveque, and B. Jecko, "New kind of microstrip antenna: The monopolar wire-patch antenna," *Electron. Lett.*, vol. 30, no. 1, Jan. 1994.

[4] S. Ramo, J. R. Whinnery, and T. Van Duzer, *Fields and Waves in Communications Electronics*, 2nd ed. New York: Wiley, 1984, p. 461.

[5] G. N. Watson, *A Treatise on the Theory of Bessel Functions*. Cambridge, U.K.: Cambridge Univ. Press, 1966, p. 73.

[6] I. Wolff and N. Knoppik, "Rectangular and circular microstrip disk capacitors and resonators," *IEEE Trans. Microwave Theory Tech.*, vol. MTT-22, pp. 857–864, Oct. 1974.

[7] R. P. Owens, "Accurate analytical determination of quasi—Static microstrip line parameters," *Radio Electron. Eng.*, vol. 46, no. 7, July 1976.

[8] J. Watkins, "Circular resonant structures in microstrip," *Electron. Lett.*, vol. 5, no. 21, pp. 524–525, Oct. 1969.

[9] R. E. Collin, *Foundation for Microwave Engineering*. New York: McGraw-Hill, 1966.

[10] T. Itoh, G. Pelosi, and P. P. Silvester, Eds., *Finite Elements Software for Microwave Engineering*. New York: Wiley, 1996.

[11] D. Kajfez and E. J. Hwan, "Q-factor measurement with network analyzer," *IEEE Trans. Microwave Theory Tech.*, vol. MTT-32, pp. 666–670, July 1984.

[12] D. Kajfez, S. Chebolu, M. R. Abdul-Gaffoor, and A. A. Kishk, "Uncertainty analysis of the transmission-type measurement of Q-factor," *IEEE Trans. Microwave Theory Tech.*, vol. 47, pp. 367–371, Mar. 1999.

Massimiliano Simeoni (S'96–M'02) was born in Rieti, Italy, on July 4, 1974. He received the Laurea degree (*summa cum laude*) from the University of Perugia, Perugia, Italy, in 1999, and the Ph.D. degree in microwave and optical communications from the University of Limoges, Limoges, France, in 2002. His thesis concerned the numerical and analytical characterization and design of new types of microwave resonators and filters.

In June 2002, he joined the European Space Research and Technology Center (ESTEC), European Space Agency (ESA), Noordwijk, The Netherlands, where he is currently a Research Fellow. His research interests include the numerical characterization of guiding structures, waveguides discontinuities, and microwave passive filter design techniques.

Roberto Sorrentino (M'77–SM'84–F'90) received the Doctor degree in electronic engineering from the University of Rome "La Sapienza," Rome, Italy, in 1971.

In 1971, he joined the Department of Electronics, University of Rome "La Sapienza," where he became an Assistant Professor in 1974. He was also Professore Incaricato with the University of Catania (1975–1976), the University of Ancona (1976–1977), and the University of Rome "La Sapienza" (1977–1982), where he was then an Associate Professor (1982–1986). In 1983 and 1986, he was a Research Fellow with The University of Texas at Austin. From 1986 to 1990, he was a Professor with the Second University of Rome "Tor Vergata." Since November 1990, he has been a Professor with the Università di Perugia, Perugia, Italy, where he was the Chairman of the Electronic Institute, Director of the Computing Center, and is currently the Dean of the Faculty of Engineering. His research activities have been concerned with EM-wave propagation in anisotropic media, interaction with biological tissues, and mainly with the analysis and design of microwave and millimeter-wave passive circuits. He has contributed to the planar-circuit approach for the analysis of microstrip circuits and to the development of numerical techniques for the modeling of components in planar and quasi-planar configurations. He is an Editorial Board member for the *International Journal of Numerical Modeling* and the *International Journal of Microwave and Millimeter-Wave Computer-Aided Engineering*.

Dr. Sorrentino is currently an Editorial Board member for the IEEE TRANSACTIONS ON MICROWAVE THEORY AND TECHNIQUES.

Serge Verdeyme (M'99), photograph and biography not available at time of publication.